Solar Physics (2006) 238: 313–327
DOI: 10.1007/s11207-006-0215-1

TRANSITION-REGION EXPLOSIVE EVENTS: RECONNECTION MODULATED BY *p*-MODE WAVES

P.F. CHEN
Department of Astronomy, Nanjing University, Nanjing 210093, China; Mathematical Institute, University of St. Andrews, Fife KY16 9SS,U.K.
(e-mail: chenpf@nju.edu.cn)

and

E.R. PRIEST
Mathematical Institute, University of St. Andrews, Fife KY16 9SS, U.K.

(Received 1 May 2006; accepted 5 September 2006; Published online 26 October 2006)

Abstract. Transition-region explosive events (TREEs) have long been proposed as a consequence of magnetic reconnection. However, several critical issues have not been well addressed, such as the location of the reconnection site, their unusually short lifetime (about one minute), and the recently discovered repetitive behaviour with a period of three to five minutes. In this paper, we perform MHD numerical simulations of magnetic reconnection, where the effect of five-minute solar *p*-mode oscillations is examined. UV emission lines are synthesised on the basis of numerical results in order to compare with observations directly. It is found that several typical and puzzling features of the TREEs with impulsive bursty behaviour can only be explained if there exist *p*-mode oscillations and the reconnection site is located in the upper chromosphere at a height range of around 1900 km $< h <$ 2150 km above the solar surface. Furthermore, the lack of proper motions of the high-velocity ejection may be due to a rapid change of temperature along the reconnection ejecta.

1. Introduction

The Sun is never really quiet. Even during solar minimum, when no active regions appear on the disk, plenty of small-scale magnetic loops rooted in the network cells are subject to supergranular motions. Intranetwork fields, ephemeral fields, and the remnants of active regions from neighbouring cells merge or cancel at the network (Martin, 1988; Zhang *et al.*, 1998; Parnell, 2002), and so the "quiet" Sun is actually full of dynamics. The richness of the dynamics is implied not only by the above-mentioned magnetogram observations but also by the GOES soft X-ray light curves and UV observations (Rabin and Dowdy, 1992; Berghmans, Clette, and Moses, 1998). At UV wavelengths, several types of eruptive phenomena have been identified, such as transition-region explosive events (TREEs), spicules, and blinkers. For instance, at any one time, there are more than 30 000 TREEs in the chromospheric network across the whole Sun (Innes *et al.*, 1997).

TREEs were discovered in the UV spectra of the high-resolution telescope and spectrograph (HRTS), which indicated that UV emission lines often show

brightenings and strong Doppler shifts up to 250 km s^{-1} mainly in the network (Brueckner and Bartoe, 1983; Dere, Bartoe, and Brueckner, 1989). The lifetimes of TREEs vary between 20 and 200 seconds, with an average at 60 seconds. It was soon suggested that they are "microflares" or "nanoflares", *i.e.*, small-scale magnetic reconnection, and that a swarm of these explosive events may contribute to the quasi-steady heating of the corona (Porter *et al.*, 1987; Parker, 1988). Although the energy of TREEs alone may not be enough for coronal heating (*e.g.*, Dere, 1994), the reconnection nature of this phenomenon has been well established. First, Dere *et al.* (1991) noted that TREEs are associated with magnetic flux cancellation and their Doppler velocities are roughly equal to the Alfvén speed of the chromosphere, as required by the reconnection model. Then, Innes *et al.* (1997) found that bi-directional jets are associated with TREEs, giving a picture consistent with magnetic reconnection. Later, the relation between TREEs and photospheric magnetic field changes was found by Chae *et al.* (1998), who also emphasised the recurrence of TREEs at the same location. Such a repetitive feature was systematically studied by Ning, Innes, and Solanki (2004), who showed that at the same site TREEs tend to appear several times with typical periods of three to five minutes.

Several numerical simulations have been performed in order to understand the physical processes that are occurring during TREEs. Jin, Inhester, and Innes (1996) and Jin, Hao, and Shen (2000) presented simulations of the magnetic reconnection in the transition region, where anti-parallel field lines are driven together by a simplified supergranular motion. It was suggested that the resulting ejection of plasmoids corresponds to the observed bi-directional jets. Similar results were obtained by Karpen, Antiochos, and DeVore (1995) and Fan *et al.* (2003), and all of these authors compared the numerical results with observations qualitatively. In order to quantitatively relate the numerical results to spectral observations, Innes and Tóth (1999) made radiative MHD simulations and synthesised the corresponding UV line profiles using a simple model. They found that reconnection in the transition region can reproduce the bi-directional jets, with the upward moving jet being more extended and appearing before the downward counterpart, a feature indicated by observations. However, they could not reproduce the brightening of the UV line profile near the line centre. Roussev *et al.* (2001a–c) extensively simulated the magnetic reconnection process with parameters typical for the transition region. From the numerical results they synthesised C IV 1548 Å and O VI 1031.9 Å line profiles. Since the plasma may depart from ionisation equilibrium during the eruptive events (Sarro *et al.*, 1999), ionisation non-equilibrium effects were included in the line synthesis. They found that the emission line profiles are strongly dependent on the assumed initial state, and only with an enhanced density in the current sheet can the line profile have a core emission after the wing emission decayed, which restricted the direct comparison between their simulations and observations.

Efforts have also been taken to interpret the repetitive behaviour of TREEs. Karpen, Antiochos, and DeVore (1995), Fan *et al.* (2003), and Fan, Feng, and

Xiang (2004) explained it as the intermittency of the magnetic reconnection associated with the sporadic ejection of magnetic islands (or plasmoids) in the current sheet. However, Ning, Innes, and Solanki (2004) and Doyle, Popescu, and Taroyan (2006) found that the TREEs repeat with a quasi-period of three to five minutes, rather than randomly. Such a period is strongly suggestive of the effect of the p-mode oscillations, since they were found to be able to leak from the photosphere into the upper atmosphere along the strong magnetic tubes that are present in the network (Banerjee *et al.*, 2001; De Pontieu, Erdélyi, and James, 2004). In this paper, we perform 2.5-dimensional MHD simulations of magnetic reconnection which is modulated by the five-minute p-mode oscillations in order to try and explain the observed spectral properties and quasi-periodic recurrence of the TREEs. The numerical method is described in Section 2, numerical results are presented in Section 3, which are followed by discussions in Section 4.

2. Numerical Method

The 2.5-dimensional (*i.e.*, $\partial/\partial z = 0$) time-dependent compressible resistive MHD equations, as shown next, are numerically solved by the multi-step implicit scheme (Hu, 1989; Chen, Fang, and Hu, 2000):

$$\frac{\partial \rho}{\partial t} + \nabla \cdot (\rho \mathbf{v}) = 0, \tag{1}$$

$$\frac{\partial \mathbf{v}}{\partial t} + (\mathbf{v} \cdot \nabla)\mathbf{v} + \frac{1}{\rho}\nabla P - \frac{1}{\rho}\mathbf{j} \times \mathbf{B} + \mathbf{g} = 0, \tag{2}$$

$$\frac{\partial \psi}{\partial t} + \mathbf{v} \cdot \nabla \psi - \eta \Delta \psi = 0, \tag{3}$$

$$\frac{\partial B_z}{\partial t} + \mathbf{v} \cdot \nabla B_z + B_z \nabla \cdot \mathbf{v} - \mathbf{B} \cdot \nabla v_z - \nabla \cdot (\eta \nabla B_z) = 0, \tag{4}$$

$$\frac{\partial T}{\partial t} + \mathbf{v} \cdot \nabla T + (\gamma - 1) T \nabla \cdot \mathbf{v} - \frac{2(\gamma - 1)\eta}{\rho \beta_0}\mathbf{j} \cdot \mathbf{j} - \frac{C Q}{\rho} + H_0 = 0, \tag{5}$$

where the x- and z-axes are in the horizontal plane, and the y-axis is upward, $\gamma = 5/3$ is the ratio of specific heats, $\mathbf{g}$ is the gravitational acceleration, η is the dimensionless magnetic diffusivity, *i.e.*, inverse of the magnetic Reynolds number, $Q = \nabla \cdot [T^{5/2}(\mathbf{B} \cdot \nabla T)\mathbf{B}/B^2]$ is the field-aligned heat conduction function, and $H_0 = (C Q/\rho)_{t=0}$ is a static heating term which is imposed to maintain an initial thermal equilibrium. The seven independent variables are density (ρ), velocity (v_x, v_y, v_z), magnetic flux function (ψ), the z-component of the magnetic field (B_z) and temperature (T); note that the magnetic field ($\mathbf{B}$) is related to the magnetic flux function by $\mathbf{B} = \nabla \times (\psi \hat{\mathbf{e}}_\mathbf{z}) + B_z \hat{\mathbf{e}}_\mathbf{z}$, and $\mathbf{j} = \nabla \times \mathbf{B}$ is the current density. The equations are non-dimensionalised with the following characteristic values: $\rho_0 = 5 \times 10^{-9}\,\mathrm{kg\,m^{-3}}$,

$T_0 = 7 \times 10^3$ K, $L_0 = 500$ km, $B_0 = 18$ G. So, the characteristic plasma β_0 is 0.32, the characteristic Alfvén speed is 28 km s^{-1}, the Alfvén time scale is $\tau_A = 17.6$ seconds. The dimensionless coefficient of the heat conduction C is expressed as $C = (\gamma - 1)\kappa_0 T_0^{7/2}/(\rho_0 L_0 v_0^3)$, where $\kappa_0 = 10^{-11}$ W m^{-1} K$^{-7/2}$. In supergranules, small-scale magnetic loops are swept by convective motions to the network boundaries, where they interact with large-scale magnetic canopy. Reconnection happens at the interacting point, whose altitude is determined by the height of the small magnetic loops. Therefore, the dimensionless resistivity (η) is distributed in a localised region which is centred at (0, y_n) by means of the following expression

$$\eta = \begin{cases} \eta_m \cos(1.66\pi x)\cos[5(y - y_n)\pi], & |x| \le 0.3, |y - y_n| \le 0.1, \\ 0, & \text{elsewhere.} \end{cases} \tag{6}$$

We wish to model the anomalous resistivity excited by some micro-scale instability, but the details depend on the ratio (T_e/T_i) of electron (T_e) to ion (T_i) temperatures; this is outside the scope of the present paper and will need a two-fluid model. When $T_e \approx T_i$ we have a Buneman instability when the electron drift speed (v_e) exceeds the electron thermal speed (v_{Te}); on the other hand, when $T_e \gg T_i$ we have the ion-acoustic instability when v_e exceeds the ion thermal speed (v_{Ti}). For simplicity, in the present single-fluid model, we set η_m as

$$\eta_m = \begin{cases} \eta_0 \min(1, v_e/v_c - 1), & v_e \ge v_c, \\ 0, & \text{otherwise,} \end{cases} \tag{7}$$

where $\eta_0 = 5 \times 10^{-4}$ and v_c is the critical value of v_e, beyond which the enhanced resistivity is assumed to be excited. It is well known that the parameter-dependent resistivity model in Equation (7) can lead to fast reconnection (Tajima and Shibata, 1997). The electron drift velocity is related to the current density (j), the electron number density (n), and the electron charge (e) by $v_e = j/ne$. In dimensionless form, it is written as

$$v_e = \frac{j}{\rho}. \tag{8}$$

In order that η has the same distribution at the initial state for different cases with varying y_n, v_c is set to be the half value of v_e at the centre of the resistivity area, *i.e.*, (0, y_n). In the case $y_n = 4$, v_c is equal to 1.6.

The initial magnetic configuration is a force-free field with the form

$$\psi = \begin{cases} (2w/\pi)\cos(\pi x/2w) - 2w/\pi, & |x| < w, \\ -|x| - 2w/\pi + w, & |x| \ge w, \end{cases} \tag{9}$$

$$B_z = \begin{cases} \cos(\pi x/2w), & \text{if } |x| < w, \\ 0, & \text{if } |x| \ge w, \end{cases} \tag{10}$$

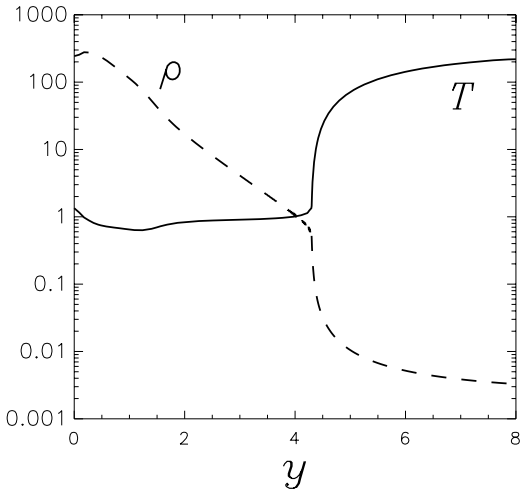

Figure 1. Distribution of dimensionless density (ρ) and temperature (T) with height (y) in the initial state.

where $w = 0.3$ is the half width of the current sheet. The initial temperature distribution from the photosphere to the upper chromosphere is set to be the same as in the VAL-3C atmospheric model for the quiet Sun (Vernazza, Avrett, and Loeser, 1981). From the upper chromosphere to the corona the temperature increases as an exponential function of the height, reaching ∼1.53 MK in the corona. The density is then calculated from the hydrostatic equilibrium equation. Figure 1 shows the initial distribution of the dimensionless temperature and density along the height.

The dimensionless size of the simulation box is $-6 \leq x \leq 6$ and $0 \leq y \leq 8$. Because of the symmetry, the calculation is made only in the right half region. The simulation domain is discretised by 112×321 grid points, which are non-uniformly spaced in both directions, being concentrated across the current sheet (in the x-direction) and the chromosphere–transition region interface (in the y-direction). Symmetry conditions are used for the left boundary ($x = 0$). The top ($y = 8$) and the right-hand side ($x = 6$) are treated as open boundaries. To simulate the well-known five-minute photospheric oscillations, a vertical velocity $v_y = 0.02 \sin(2\pi t/300)\,\mathrm{km\,s^{-1}}$ is imposed at the bottom, where other quantities are fixed. For comparison, the case with a static bottom boundary is also simulated.

In order to compare the numerical simulations with observations, we synthesise the light curve for the O VI 1031.9 Å line and spectra for the Si IV 1392 Å line from the numerical results using the CHIANTI database (Dere *et al.*, 1997; Landi *et al.*, 2006). For the light curve, the total O VI flux is computed by

$$I = \int\int \rho^2 G(T)\,\mathrm{d}x\,\mathrm{d}y, \tag{11}$$

where the integration is taken over the region $|x| \leq 0.5, 0 \leq y \leq 8$. For the spectra, the Si IV 1392 Å line profiles are computed by

$$I_\lambda = \int \rho^2 \varepsilon_T \left(\lambda - \frac{v}{c}\lambda_0\right) \mathrm{d}l, \tag{12}$$

where the integration is taken along the line of sight, v is the line-of-sight velocity, c is the light speed, and $\lambda_0 = 1392$ Å. Both the emission contribution function $G(T)$ in Equation (11) and the static line profile $\varepsilon_T(\lambda)$ in Equation (12) are obtained from the CHIANTI database.

3. Numerical Results

If magnetic field diffuses (without advection) in a local region where the resistivity is introduced, a current sheet becomes thicker. However, in our experiment, where advection is also present we find in Figure 2 that the sheet instead becomes thinner. The resulting current density enhancement makes the anomalous resistivity increase further, which finally leads to fast reconnection. Similar behaviour is found by Magara *et al.* (1996). Figure 2 depicts the evolution of the temperature, the magnetic field, and the velocity in the case where the resistivity area is centralised at $y_n = 4$ and no photospheric oscillation is imposed. Since the reconnection X-point is located in the upper chromosphere, the (relatively) cold plasmas in the reconnection inflow regions converge towards the X-point, and the heated plasmas are ejected upward and downward, with the upward velocity being significantly larger than the downward one since the corona is much more rarefied than is the dense lower atmosphere. The evolution is quite stable, although, as the recon-

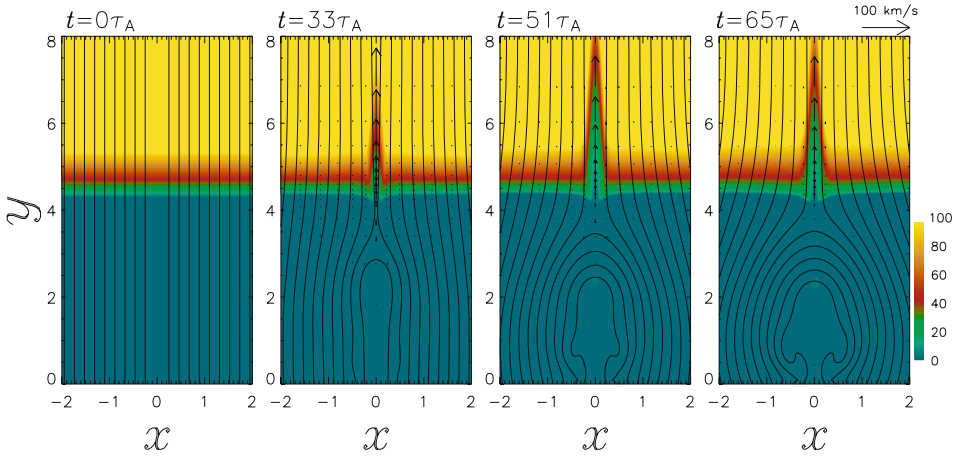

Figure 2. Evolution of the temperature (*colour*), magnetic field (*solid lines*), and velocity (*arrows*) in the case without *p*-mode oscillations.

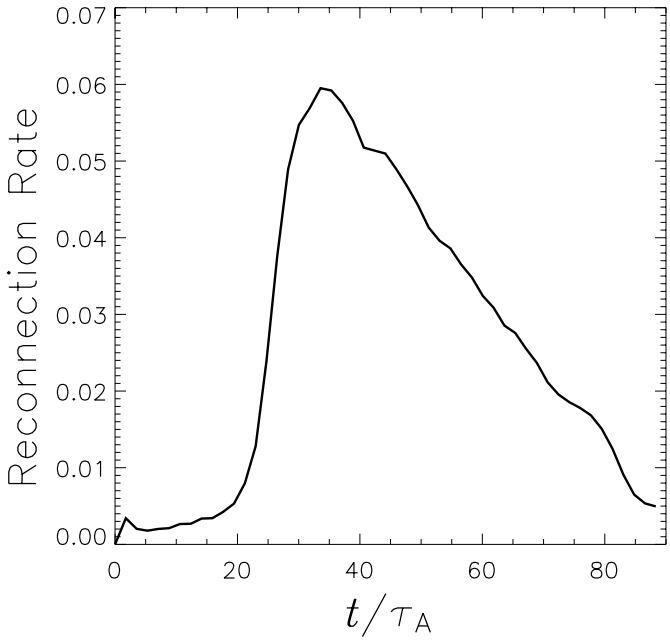

Figure 3. Time profiles of the reconnection rate (R) in the case without p-mode oscillations.

nected magnetic field lines accumulate in the lower atmosphere, a larger and larger closed-loop system grows and hinders the reconnection inflow from converging to the X-point, so that the reconnection slows down. When the closed-loop system reaches the height of the resistivity area, the reconnection then stops, as discussed by Chen *et al.* (1999) and Chen, Fang, and Ding (2001). The time variation of the reconnection rate is shown in Figure 3, where we can see that the reconnection rate decreases to a tenth of its maximum at $t = 88\tau_A$. Although the evolution of the reconnection rate is quite smooth, the synthesised O VI 1031.9 Å light curve presents a significant periodic behaviour, as shown in the left panel of Figure 4. The right panel shows the corresponding wavelet spectrum, which is obtained by the method described by Torrence and Compo (1998). The green region indicates the locations of the highest power, and the cross-hatched region corresponds to the cone of influence. It is seen that the UV light curve oscillates with a period of around three minutes.

When p-mode oscillations are imposed at the bottom boundary, the whole atmospheric begins to oscillate up and down in a way that has been modelled by Carlsson and Stein (1998), and so the reconnection proceeds in a periodic way. Figure 5 shows the evolution of the temperature, the magnetic field, and the velocity, where it is seen that the plasma jets with the transition region temperature (*green*) are ejected into the corona intermittently. The corresponding temporal variation of the reconnection rate is plotted in Figure 6, where it is seen that the reconnection rate

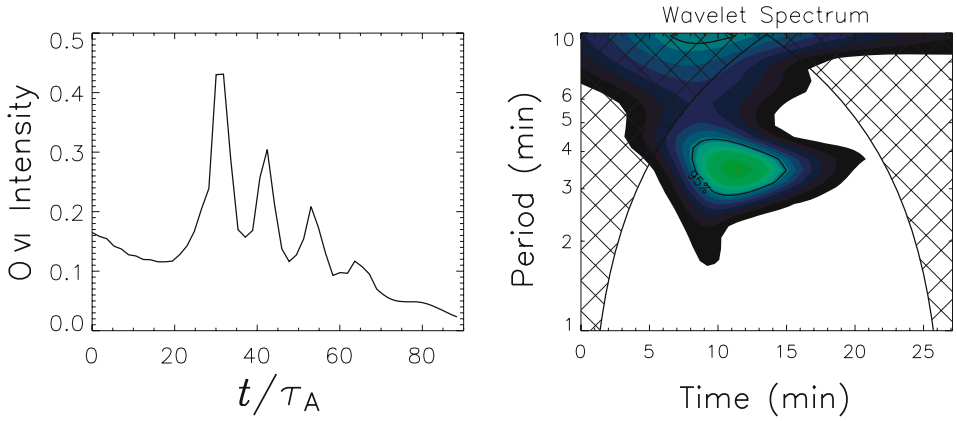

Figure 4. Time variation of the O VI 1031.9 Å emission flux (*left panel*) and its wavelet spectrum (*right panel*) in the case when no *p*-mode oscillations are imposed at the base. The right panel indicates that the light curve in the left panel has a period of around three minutes.

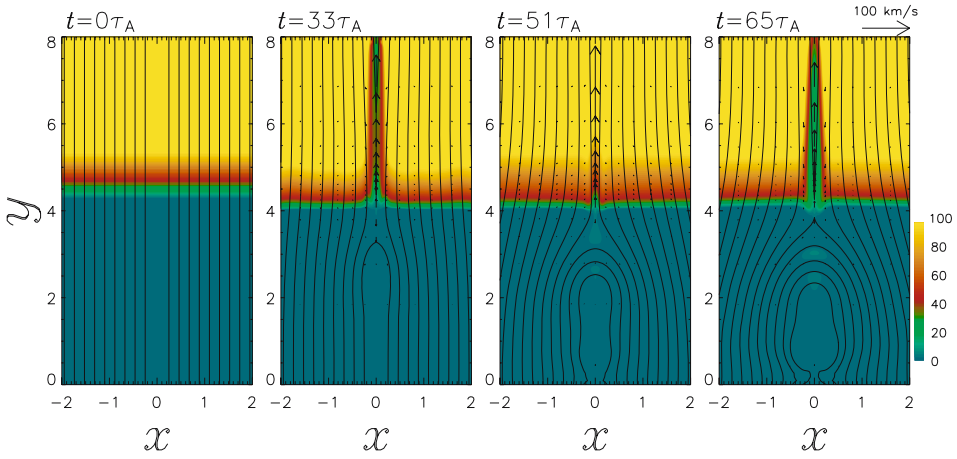

Figure 5. Evolution of the temperature (*colour*), magnetic field (*solid lines*), and velocity (*arrows*) in the case with *p*-mode oscillations imposed at the base.

is modulated with a period of roughly five minutes. With the CHIANTI database, the MHD numerical results in Figure 5 are converted into Si IV 1392 Å line emissions. Suppose that the reconnection process is observed by a slit spectrometer with a line of sight 20° inclined to the normal direction of the solar surface. The corresponding slit spectra are illustrated in Figure 7, where the velocity (or equivalently wavelength) is along the horizontal direction and the slit is along the vertical direction. It is seen that the brightenings are generally limited to a typical spatial size less than one arcsec. From the upward reconnection jet to the downward one, the Si IV 1392 Å line profiles change from being predominant in the blue wing to

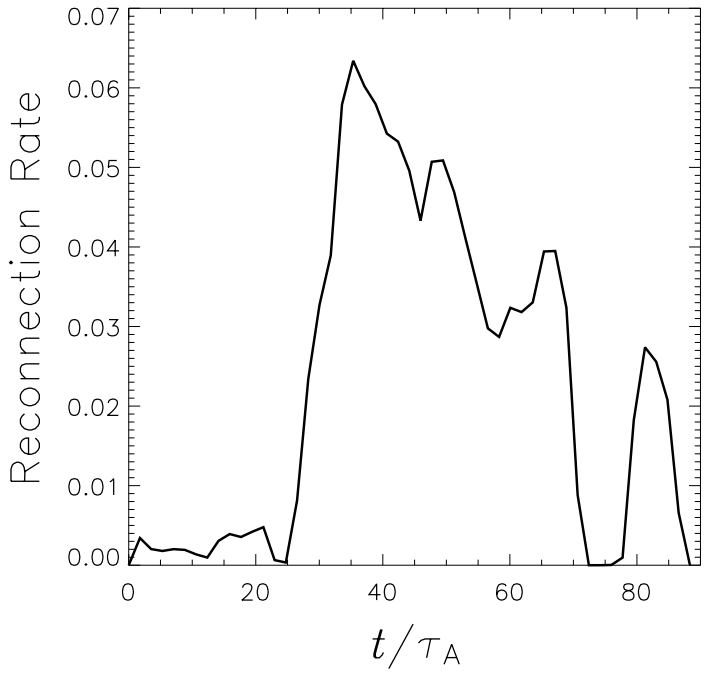

Figure 6. Time profile of the reconnection rate (R) in the case with p-mode oscillations imposed at the base.

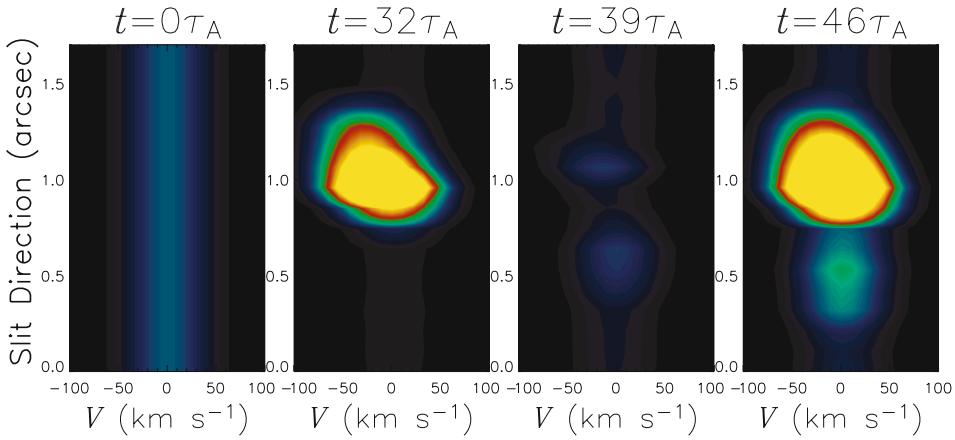

Figure 7. Evolution of the Si IV 1392 Å slit spectra of the numerical results in the case with p-mode oscillations imposed at the base.

being slightly shifted towards the red wing, and the slit spectra are significantly biased towards the blue wing. Another important characteristic in Figure 7 is that the brightenings appear repeatedly. Such a repetitive behaviour can be easily discerned in the total O VI 1031.9 Å light curve, which is plotted in the left panel of

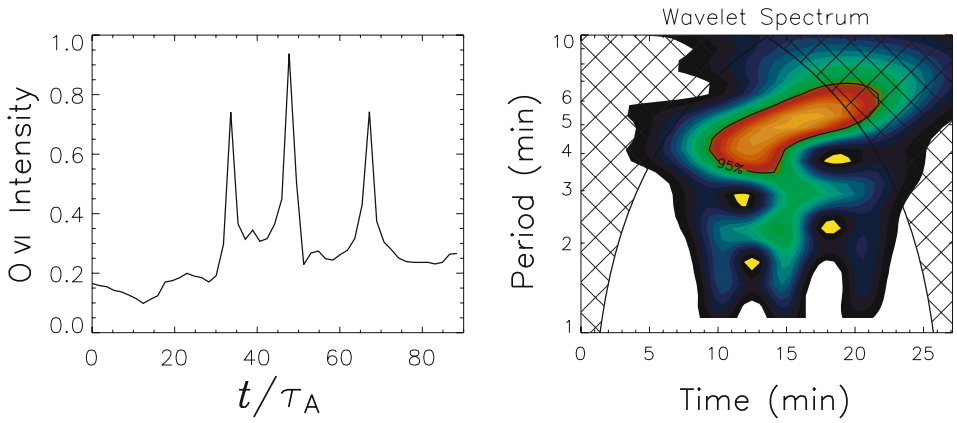

Figure 8. Time variation of the O VI 1031.9 Å emission flux (*left panel*) and its wavelet spectrum (*right panel*) when *p*-mode oscillations are imposed at the base. The right panel indicates that the light curve in the left panel has a period increasing from about three minutes to more than five minutes.

Figure 8. The wavelet spectrum in the right panel, where the red region indicates the locations of the highest power, indicates that the explosive events repeat with a period increasing from around three minutes to more than five minutes, a result which is also seen in the observations (Doyle, Popescu, and Taroyan, 2006).

When the resistivity area is centred within $3.8 \leq y_n \leq 4.5$, the reconnection and the corresponding EUV light curves show similar significant oscillations. As the resistivity area is moved further away from this range, however, either upward or downward, the repetitive behaviour becomes less and less pronounced.

4. Discussion

TREEs were found to be associated with magnetic cancellation (Dere *et al.*, 1991), which was strongly suggestive of the presence of magnetic reconnection. The discovery of bi-directional jets associated with TREEs further confirmed that magnetic reconnection is responsible for the transient brightenings (Innes *et al.*, 1997). Thereafter, several numerical simulations of the magnetic reconnection have been conducted in order to explain the observational features. For example, the predominant blue shift component of their UV lines has been attributed to the highly stratified atmosphere (Innes and Tóth, 1999; Roussev *et al.*, 2001c). Despite this progress, several key points still need to be addressed about the reconnection model. Firstly, there is a lack of proper motion of the high Doppler-velocity brightenings; secondly, the UV line profiles have not been well reproduced, in particular the line-centre emission; thirdly, their lifetime is unusually short. Finally, TREEs often repeat with a quasi-period, rather than randomly.

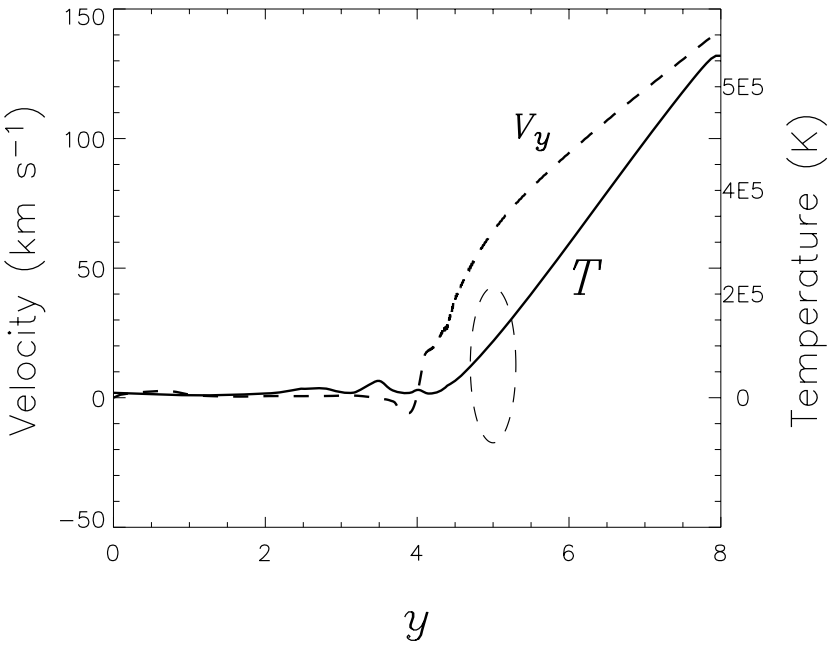

Figure 9. Distribution of the temperature (T, *solid line*) and the y-component of the velocity (v_y, *dashed line*) along the y-axis at $t = 53\tau_A$. The *dashed ellipse* indicates the location that contributes substantially to Si IV emission.

4.1. PROPER MOTIONS AND CENTRAL EMISSIONS

One aspect of the observed properties of TREEs that was hard to explain is the lack of detectable apparent motion of the high-velocity emission across the slit or the solar surface (Dere, Bartoe, and Brueckner, 1989). This feature has been thought by many to be inconsistent with an outgoing reconnection jet.

The absence of a proper motion of the Doppler-shifted emissions in TREEs has now been reproduced in our new numerical experiment: Figure 7 indicates that the emission site stays roughly at the same location, despite the large speed of the reconnection outflow, $v \sim 100\,\mathrm{km\,s^{-1}}$, as illustrated by the arrows in Figure 5. This can be explained as follows. The combination of thermal conduction and the static heating term (H_0) makes the temperature of the reconnection outflow vary rapidly during the ejection. As an example, Figure 9 depicts the temperature and the upward velocity distributions along the y-axis at $t = 53\tau_A$ for the case where $y_n = 4$. Only the portion with T around 6.3×10^4 K, as highlighted by the ellipse in the figure, contributes significantly to the Si IV 1392 Å emission. As the plasma moves up, its temperature increases, and so it becomes invisible in Si IV 1392 Å. (It is noted that in a more general three-dimensional case, the reconnection jet may also experience a rotating motion as reported by Pike and Mason (1998), which

is guided by the helical field lines as proposed by Harrison, Bryans, and Bingham (2001) and Whitelam *et al.* (2002).)

Another issue regarding the reconnection model is the reproduction of the spectral profiles of the EUV emission lines. Innes (2001) can reproduce the Doppler-shifted wing emissions, but not the brightening near the line centre. Roussev *et al.* (2001c) found that the line centre can be bright only in the late phase of the case where there is a density concentration along the vertical current sheet. The problem could be simply due to the much simplified initial atmospheric model in their work. In this paper, with an initial temperature distribution adopted from the quiet Sun atmospheric model, *i.e.*, the VAL-3C model (Vernazza, Avrett, and Loeser, 1981), the slit spectra shown in Figure 7 do indeed present the typical spectral characteristic of TREEs, *i.e.*, both the line centre and the wide wings are bright.

It should be noted that the radiative cooling time scale in the low-layer solar atmosphere is of the order of the heating or conduction time scales, and so radiative cooling is important in the dynamic evolution, but it has been neglected in this paper for the sake of simplicity. The effect of radiative cooling on the reconnection process and the spectral properties will be studied in a future paper.

4.2. Short lifetime and repetitive behaviour of TREEs

If magnetic reconnection, specifically in the upper chromosphere as found in this paper, is responsible for the TREE phenomenon, a big puzzle arises since Chen *et al.* (1999) found that owing to the line-tying effect, reconnected field lines below the reconnection X-point accumulate to form an expanding quasi-potential loop system, which rises eventually to the X-point and stops the reconnection. The lifetime of reconnection is approximately proportional to the height of the reconnection X-point. If such spontaneous reconnection happens in the chromosphere, the lifetime is typically 10 to 15 minutes (Chen, Fang, and Ding, 2001), which is much longer than the typical lifetime of TREEs, *i.e.*, 60 seconds. The discrepancy between these two time scales can, however, be reconciled if the reconnection is modulated.

It has long been noticed that TREEs appear in bursts (Dere, 1994; Chae *et al.*, 1998; Pérez *et al.*, 1999). Recently, Ning, Innes, and Solanki (2004) found that they repeat with periods of three to five minutes. Doyle, Popescu, and Taroyan (2006) further pointed out that the TREE occurrence rate increases from around three minutes to over five minutes at a single site. They interpreted it in terms of a kink mode of the flux tube.

The bursty behaviour of TREEs was interpreted as the successive ejections of plasmoids (or magnetic islands; Karpen, Antiochos, and DeVore, 1995; Fan *et al.*, 2003). However, as pointed out by Doyle, Popescu, and Taroyan (2006), it is difficult for this model to explain the quasi-periodicity. The five-minute repetition is strongly reminiscent of the dominant *p*-mode helioseismic periods. Using a fairly realistic atmospheric model in this paper, simulations of magnetic reconnection are

performed in two cases: (1) the photospheric base is fixed; (2) five-minute oscillations are imposed at the photospheric base. When the photospheric base is fixed, the reconnection proceeds quasi-steadily, and the reconnection rate evolves smoothly. The synthesised UV light curve oscillates with a period of around three minutes only. However, when five-minute p-mode waves are imposed at the photospheric base, the solar atmosphere oscillates accordingly. It turns out that the reconnection rate is modulated with a period of roughly five minutes. The corresponding UV light curve indicates that the explosive events appear repetitively with a period increasing from around three minutes to more than five minutes, with each episode having spiky bursts that last only about 60 seconds as indicated in the left panel of Figure 8. In other words, only when the reconnection is modulated by the five-minute p-mode oscillations, the synthesised UV explosive events can reproduce the above-mentioned typical observational features of TREEs.

The coupling between the reconnection and the p-mode waves can be understood as follows. As the solar atmosphere oscillates, the plasma density near the reconnection site varies in time accordingly, which results in a periodic variation of the electron drift speed (v_e in Equation (8)) even when the current density (j) is quasi-constant. Since the resistivity is strongly dependent on v_e, the reconnection rate oscillates accordingly, with several peaks during the evolution when the local density near the reconnection site is low (hence the resistivity is high), as shown in Figure 6. The O VI 1031.9 Å emission shows a spike only when the reconnection rate reaches a peak. At the same time, when the density near the reconnection X-point is low, the Alfvén velocity in the inflow region becomes high. Therefore, the ejecta achieves a velocity of the order of $100\,\mathrm{km\,s^{-1}}$ even though the Alfvén velocity at the height $y = 4$ is about $28\,\mathrm{km\,s^{-1}}$ under the initial conditions. With a stronger magnetic field, a faster ejecta is expected. It is noted that although the UV flux appears in separate bursts, which returns to the quiescent level between the bursts, the reconnection rate remains rather high even between the explosive events. This explains the observations that the local photospheric magnetic flux continuously decreases even though the explosive events occur in bursts (Chae *et al.*, 1998).

When the five-minute p-mode oscillations are imposed at the photospheric base, the wavelet spectrum of the O VI 1031.9 Å emission in the right panel of Figure 8 indicates that the explosive events do appear in a quasi-periodic way, with the period increasing from around three minutes to over five minutes, exactly as was discovered by Doyle, Popescu, and Taroyan (2006). The five-minute period, which was expected, can be easily understood to be due to the five-minute p-mode oscillations. The unexpected shorter period starting from around three minutes instead results from standing slow-mode waves in the chromospheric resonator as described by Chen *et al.* (2006, in preparation). This is why the three-minute periodicity is also present in the case when no p-mode oscillations are imposed at the photospheric base.

It is found that when the reconnection site is in the range of $3.8 \leq y_n \leq 4.3$ (which corresponds to a real height between 1900 and 2150 km in the quiet Sun

atmosphere), the O VI light curves show such a repetitive behaviour, with each episode lasting about one minute. When the reconnection site is lower, the oscillation amplitude induced by the p-mode becomes smaller, its modulation to the reconnection rate becomes weaker and weaker, and the UV light curves tend to be smoother and smoother. On the other hand, when the reconnection site is higher, the plasma β becomes smaller and smaller, so that the reconnection process is dominantly controlled by the intrinsic MHD dynamics and is less and less affected by the p-mode oscillations. The lifetime of the reconnection also becomes longer and longer. This may explain some long-lifetime (>40 minutes) explosive events as reported by Porter *et al.* (1987). If the reconnection point is located further up in the low corona, the dynamics would correspond to X-ray bright points (Priest, Parnell, and Martin, 1994; Parnell and Priest, 1995; von Rekowski, Parnell, and Priest, 2006).

It is noted in passing that magnetic cancellation in the photospheric magnetograms is often argued to be direct evidence of the magnetic reconnection during the TREEs. However, our numerical simulations indicate that actually the photosphere is often dense enough to stop the reconnected flux loops from submerging. Perhaps photospheric magnetic cancellation occurs when the reconnected flux loops are subject to downward supergranular motions within the network. Only when the reconnected flux is swept down by the convective motions, the reconnection can proceed for a longer time, and up to seven bursts may be seen at one site as observed by Ning, Innes, and Solanki (2004).

Acknowledgements

This research is supported by the Chinese foundations NCET-04-0445, FANEDD (200226), 2006CB806302, NSFC (10221001, 10333040 and 10403003), and by the UK Particle Physics and Astronomy Research Council.

References

Banerjee, D., O'Shea, E., Doyle, J.G., and Goossens, M.: 2001, *Astron. Astrophys.* **371**, 1137.
Berghmans, D., Clette, F., and Moses, D.: 1998, *Astron. Astrophys.* **336**, 1039.
Brueckner, G.E. and Bartoe, J.-D.F.: 1983, *Astrophys. J.* **272**, 329.
Carlsson, M. and Stein, R.F.: 1998, in F. Deubner, J. Christensen-Dalsgaard, and D. Kurtz (eds.), *New Eyes to See Inside the Sun and the Stars*, IAU Symposium, Kyoto, Japan, **185**, p. 435.
Chae, J., Wang, H., Lee, C., Goode, P.R., and Schühle, U.: 1998, *Astrophys. J.* **497**, L109.
Chen, P.F. *et al.*: 2006, in preparation.
Chen, P.F., Fang, C., and Ding, M.D.: 2001, *Chin. J. Astron. Astrophys.* **1**, 179.
Chen, P.F., Fang, C., and Hu, Y.Q.: 2000, *Chin. Sci. Bull.* **45**, 798.
Chen, P.F., Fang, C., Ding, M.D., and Tang, Y.H.: 1999, *Astrophys. J.* **520**, 853.
De Pontieu, B., Erdélyi, R., and James, S.P.: 2004, *Nature* **430**, 536.

Dere, K.P.: 1994, *Adv. Space Res.* **14**, 13.
Dere, K.P., Bartoe, J.-D.F., and Brueckner, G.E.: 1989, *Solar Phys.* **123**, 41.
Dere, K.P., Bartoe, J.-D.F., Brueckner, G.E., Ewing, J., and Lund, P.: 1991, *J. Geophys. Res.* **96**, 9399.
Dere, K.P., Landi, E., Mason, H.E., Monsignori Fossi, B.C., and Young, P.R.: 1997, *Astron. Astrophys. Suppl.* **125**, 149.
Doyle, J.G., Popescu, M.D., and Taroyan, Y.: 2006, *Astron. Astrophys.* **446**, 327.
Fan, Q.L., Feng, X.S., and Xiang, C.Q.: 2004, *Comm. Theor. Phys.* **41**, 790.
Fan, Q.L., Feng, X.S., Xiang, C., and Zhong, D.K.: 2003, *Phys. Plasma* **10**, 4575.
Harrison, R.A., Bryans, P., and Bingham, R.: 2001, *Astron. Astrophys.* **379**, 324.
Hu, Y.Q.: 1989, *J. Comput. Phys.* **84**, 441.
Innes, D.E.: 2001, *Astron. Astrophys.* **378**, 1067.
Innes, D.E. and Tóth, G.: 1999, *Solar Phys.* **185**, 127.
Innes, D.E., Inhester, B., Axford, W.I., and Wilhelm, K.: 1997, *Nature* **386**, 811.
Jin, S.-P., Hao, L., Shen, J.T.: 2000, *Chin. Astron. Astrophys.* **24**, 224.
Jin, S.-P., Inhester, B., and Innes, D.E.: 1996, *Solar Phys.* **168**, 279.
Karpen, J.T., Antiochos, S.K., and DeVore, C.R.: 1995, *Astrophys. J.* **450**, 422.
Landi, E., Del Zanna, G., Young, P.R., Dere, K.P., Mason, H.E., and Landini, M.: 2006, *Astrophys. J. Suppl.* **162**, 261.
Magara, T., Mineshige, S., Yokoyama, T., and Shibata, K.: 1996, *Astrophys. J.* **466**, 1054.
Martin, S.F.: 1988, *Solar Phys.* **117**, 243.
Ning, Z., Innes, D.E., and Solanki, S.K.: 2004, *Astron. Astrophys.* **419**, 1141.
Parker, E.N.: 1988, *Astrophys. J.* **330**, 474.
Parnell, C.E.: 2002, *Mon. Not. Roy Astron. Soc.* **335**, 389.
Parnell, C.E. and Priest, E.R.: 1995, *Geophys. Astrophys. Fl. Dyn.* **80**, 255.
Pérez, M.E., Doyle, J.G., Erdélyi, R., and Sarro, L.M.: 1999, *Astron. Astrophys.* **342**, 279.
Pike, C.D. and Mason, H.E.: 1998, *Solar Phys.* **182**, 333.
Porter, J.G., Moore, R.L., Reichmann, E.J., Engvold, O., and Harvey, K.L.: 1987, *Astrophys. J.* **323**, 380.
Priest, E.R., Parnell, C.E., and Martin, S.F.: 1994, *Astrophys. J.* **427**, 459.
Rabin, D. and Dowdy, J.F., Jr.: 1992, *Solar Phys.* **398**, 665.
Roussev, I., Galsgaard, K., Erdélyi, R., and Doyle, J.G.: 2001a, *Astron. Astrophys.* **370**, 298.
Roussev, I., Galsgaard, K., Erdélyi, R., and Doyle, J.G.: 2001b, *Astron. Astrophys.* **375**, 228.
Roussev, I., Doyle, J.G., Galsgaard, K., and Erdélyi, R.: 2001c, *Astron. Astrophys.* **380**, 719.
Sarro, L.M., Erdélyi, R., Doyle, J.G., and Perez, E.P.: 1999, *Astron. Astrophys.* **351**, 721.
Tajima, T. and Shibata, K.: 1997, *Plasma Astrophysics*, Addison-Wesley, Reading, MA.
Torrence, C. and Compo, G.P.: 1998, *Bull. Am. Meteorol. Soc.* **79**, 61.
Vernazza, J.E., Avrett, E.H., and Loeser, R.: 1981, *Astrophys. J. Suppl.* **45**, 635.
von Rekowski, B., Parnell, C.E., and Priest, E.R.: 2002, *Mon. Not. R. Astron. Soc.* **366**, 125.
Whitelam, S., Ashbourn, J.M.A., Bingham, R., Shukla, P.K., and Spicer, D.S.: 2002, *Solar Phys.* **211**, 199.
Zhang, J., Lin, G., Wang, J., Wang, H., and Zirin, H.: 1998, *Solar Phys.* **338**, 322.